Published in final edited form as:
Cancer Res. 2014 January 1; 74(1): 309–319. doi:10.1158/0008-5472.CAN-12-4721.

ERK1/2 BLOCKADE PREVENTS EPITHELIAL-MESENCHYMAL TRANSITION IN LUNG CANCER CELLS AND PROMOTES THEIR SENSITIVITY TO EGFR INHIBITION

Janine M. Buonato[1] and **Matthew J. Lazzara**[1,2]

[1]Department of Chemical and Biomolecular Engineering, University of Pennsylvania, Philadelphia, PA 19104

[2]Department of Bioengineering, University of Pennsylvania, Philadelphia, PA 19104

Abstract

Overcoming cellular mechanisms of *de novo* and acquired resistance to drug therapy remains a central challenge in the clinical management of many cancers, including non-small cell lung cancer (NSCLC). While much work has linked the epithelial-mesenchymal transition (EMT) in cancer cells to the emergence of drug resistance, it is less clear where tractable routes may exist to reverse or inhibit EMT as a strategy for drug sensitization. Here, we demonstrate that ERK1/2 (MAPK3/1) signaling plays a key role in directing the mesenchymal character of NSCLC cells, and that blocking ERK signaling is sufficient to heighten therapeutic responses to EGFR inhibitors. MEK1/2 (MAPKK1/2) inhibition promoted an epithelial phenotype in NSCLC cells, preventing induction of EMT by exogenous TGFβ. Moreover, in cells exhibiting *de novo* or acquired resistance to the EGFR inhibitor gefitinib, MEK inhibition enhanced sensitivity to gefitinib and slowed cell migration. These effects only occurred, however, if MEK was inhibited for a period sufficient to trigger changes in EMT marker expression. Consistent with these findings, changes in EMT phenotypes and markers were also induced by expression of mutant KRAS in a MEK-dependent manner. Our results suggest that prolonged exposure to MEK or ERK inhibitors may not only restrain EMT but overcome naïve or acquired resistance of NSCLC to EGFR-targeted therapy in the clinic.

INTRODUCTION

Epidermal growth factor receptor (EGFR) over-expression and -activation are hallmarks of many cancers, including non-small cell lung cancer (NSCLC). Consequently, a number of inhibitors and monoclonal antibodies targeting EGFR have been developed and approved for various cancers. Unfortunately, these drugs are generally ineffective. In NSCLC, response to EGFR inhibitors is limited mainly to the rare patients (~10%) whose tumors harbor somatic, kinase-activated mutants of EGFR (1, 2). Even these patients almost invariably develop resistance to EGFR inhibitors, often through the EGFR “gatekeeper” mutation (T790M) (3, 4) or through up-regulation of c-MET or other receptors (5). Combination therapies present a possible strategy to overcome resistance. In NSCLC, recent investigations suggest promise for combining EGFR inhibitors with chemoradiation (6), the multi-kinase inhibitor sorafenib

Corresponding Author: Matthew J. Lazzara, Department of Chemical and Biomolecular Engineering, University of Pennsylvania, 311A Towne Building, 220 South 33rd Street, Philadelphia, PA 19104-6393, (p) 215-746-2264, (f) 215-573-2093, mlazzara@seas.upenn.edu.

Conflicts of Interest
The authors declare no conflicts of interest.

(7), or a c-MET inhibitor (8). Scheduling multiple drugs such that initial therapy reprograms cells to respond to another drug is another possible strategy. In one recent example, triple-negative breast cancer cells and NSCLC cells were dramatically sensitized to doxorubicin by pretreatment with the EGFR inhibitor erlotinib (9).

Epithelial-mesenchymal transition (EMT) is another pathway through which cancers of epithelial origin become chemoresistant. EMT is a developmental process whereby epithelial cells lose cell-cell adhesions to become more motile and invasive. Cells undergoing EMT lose expression of epithelial markers (e.g., E-cadherin) and gain expression of mesenchymal markers (e.g., vimentin and fibronectin) through differential expression and activation of transcription factors including Twist, ZEB1, and Snail (10, 11). EMT is frequently hijacked in metastatic progression, and mesenchymal dedifferentiation has been associated with resistance to EGFR inhibitors, chemotherapy, and other targeted drugs in cancers of the lung (12–14), bladder (15), head and neck (16, 17), pancreas (18), and breast (19). In NSCLC, *in vitro* acquired resistance to the EGFR inhibitor erlotinib can result from selection of a mesenchymal sub-population (20), and restoring E-cadherin expression in mesenchymal-like NSCLC cells potentiates sensitivity to EGFR inhibitors (21). Additionally, growing evidence for AXL-mediated EGFR inhibitor resistance has been tied to EMT (22). Thus, developing treatments that elicit a mesenchymalepithelial transition (MET) could be a useful approach for expanding the efficacy of EGFR inhibitors.

Several studies have demonstrated a requirement for extracellular signal-regulated kinase-1/2 (ERK1/2, or MAPK3/1) pathway activity in EMT induced by transforming growth factor beta (TGFβ) in non-transformed cells (23–25). ERK2, but not ERK1, activity also induces EMT in non-transformed mammary epithelial cells (26) and has been implicated as mediating oncogenic KRAS-induced invasion in pancreatic cancer cells (27). Interestingly, *ERK2* amplification was recently identified as a mechanism leading to acquired resistance to EGFR inhibitors in NSCLC (28).

Here, we sought to determine ERK's role in governing EMT in NSCLC. In a panel of NSCLC cell lines, inhibition of MEK1/2 (MAPKK1/2) prevented TGFβ-induced EMT and promoted epithelial cellular characteristics when administered alone. Conversely, augmented ERK activation, through $KRAS^{12V}$ expression or *ERK2* amplification, promoted mesenchymal characteristics. Furthermore, chronic MEK inhibition for times long enough to observe changes in epithelial and mesenchymal marker expression augmented cellular sensitivity to the EGFR inhibitor gefitinib in cell lines with *de novo* or acquired resistance to EGFR inhibitors. These changes were reversible and accompanied by shifts in expression of stem cell-like markers CD24 and CD44. These results suggest the potential utility of drug scheduling strategies first targeting ERK to promote epithelial characteristics prior to targeting EGFR or other oncogenic signaling nodes.

MATERIALS AND METHODS

Cell culture

H1666 cells were obtained from the American Type Culture Collection. H322, gefitinib-resistant PC9 (clone GR4, referred to as GR henceforth), and WZ4002-resistant PC9 cells (clone WZR12, referred to as WZR henceforth) were provided by Dr. Pasi Jänne (Dana-Farber Cancer Institute). Parental PC9 cells were provided by Dr. Douglas Lauffenburger (MIT). Since PC9 cells came from different labs, we confirmed similar expression of important proteins and response to gefitinib for parental stocks from both labs. H358 cells were provided by Dr. Russ Carstens (University of Pennsylvania). PC9 (all variants), H322, and H358 cells were maintained in RPMI 1640 supplemented with 10% FBS, 100 units/mL penicillin, 100 μg/mL streptomycin, and 1 mM L-glutamine. H1666 cells were maintained in

ACL4 (29). Cell culture reagents were from Life Technologies. Cell lines were validated for anticipated responsiveness to gefitinib and were cultured for less than two months from low-passage frozen stocks.

Chronic MEK inhibition

H1666, PC9 GR, and PC9 WZR cells were maintained in 10 μM, 5 μM, and 20 μM U0126, respectively, with controls maintained in DMSO. Responses to 1 hr or 2 day treatments with a range of U0126 concentrations were evaluated for each cell line to identify U0126 concentrations yielding significantly inhibited ERK phosphorylation (Supplementary Fig. S1) but minimal background cell death. For culture experiments, media was changed every two days or cells were passed as necessary. When passing, cells were sub-cultured into inhibitor-free media to promote adhesion. U0126 or DMSO was replaced the following day. When appropriate, cells were lysed or gefitinib was added 24 hrs later. Time points in figures with chronic MEK inhibition reflect the total time of U0126 exposure before lysing or gefitinib addition. To probe the reversibility of U0126 effects, cells were split from U0126 cultures after 7 days and maintained in DMSO thereafter. All time courses were performed from freshly thawed cells multiple times to demonstrate reproducibility. Naïve cell death response to U0126 and gefitinib was quantified at multiple points during time courses, including the beginning and end, to verify that baseline response was not changing.

Wound healing assay

Confluent cell monolayers in 6-well plates were scratched with a pipet tip, and media was immediately changed. Phase contrast images were taken with a Zeiss Axiovert 40 CFL microscope (10X objective) every 1–3 hrs for ≤11 hrs. Scratch areas were quantified using ImageJ, and closure rates were calculated from linear fits of areas versus time and reported as percent of total image area closed per hr normalized to the conditions indicated in figures. Where inhibitors were used, cells were plated at sub-confluence and treated at appropriate times with media containing inhibitor. Media and inhibitor were changed every two days until wells reached confluence.

Transwell migration assay

Untreated PC9 GR and WZR cells or H1666 cells treated with U0126 or DMSO for 4 days were trypsinized and resuspended in media containing 0.1% FBS and U0126 or DMSO for H1666. 20,000 untreated or DMSO-treated cells or 50,000 U0126-treated cells (adjusted for U0126-mediated changes in adhesion) were added to 8 μm Transwell membranes (Corning), which were placed in 24-well plates well containing complete media with DMSO or U0126. After 20 hrs, cells on the upper surfaces were removed with a cotton swab. Cells on the lower surfaces were fixed in 4% paraformaldehyde for 30 min and washed with PBS, and nuclei were stained with Hoescht-33342. Membranes were mounted and imaged (10X objective), and nuclei were counted using ImageJ. Counts were normalized to the number of adhered cells from parallel wells for each condition.

Flow cytometry

For cell death assays, cells were plated in 6-well dishes from their various culture conditions and treated with inhibitors. Floating and adherent cells were collected 48 hrs later, resuspended in PBS containing TO-PRO3 (Life Technologies), and analyzed within 1 hr. For CD24 and CD44 measurements, cells were collected as above, washed with 0.1% BSA in PBS (PBSA), blocked for 10 min in PBSA, and incubated for 1 hr with 3 μL each of FITC-conjugated anti-human CD44 antibody (BD Pharmingen, #555478) and Alexa-647 conjugated anti-human CD24 antibody (BioLegend, #311109) in 200 μL. Labeled cells were

washed again and resuspended in PBS. Cytometry was performed on a BD Biosciences FACSCalibur cytometer, and data were analyzed using FlowJo.

Antibodies and other reagents

pERK T202/Y204 (#4377) and ERK (#4695) antibodies were from Cell Signaling Technology. E-cadherin (sc-8426), vimentin (sc-373717), fibronectin (sc-8422), and GAPDH (sc-32233) antibodies were from Santa Cruz Biotechnology. Stocks of U0126 and gefitinib (LC Labs) were prepared in DMSO. Recombinant human epidermal growth factor (EGF) and TGFβ were from Peprotech. Infrared dye- and Alexa Fluor®-conjugated secondary antibodies were from Rockland Immunochemicals and Invitrogen, respectively.

Additional methods

Western blotting, immunofluorescence, $KRAS^{12V}$ expression, experiments involving CI-1040, chronic MEK inhibition in H322, H358, and SKRB3 cells, and the EGFR internalization assay were performed as described in Supplemental Materials.

RESULTS

NSCLC cell lines undergo MEK-dependent TGFβ-induced EMT

H1666, H322, and H358 cells were cultured in complete media with TGFβ and EGF with or without U0126 for four days, with a media change after two days (Fig. 1). In response to TGFβ and EGF, E-cadherin expression decreased and vimentin expression increased in all three cell lines, and fibronectin expression increased in H1666 and H358 cells (Fig. 1A). U0126 co-treatment inhibited changes in E-cadherin and vimentin, but did not prevent fibronectin induction. The same trends were found in H1666 cells using the alternative MEK inhibitor CI-1040 (Supplementary Fig. S2). The conditions used in Fig. 1A were explored in H1666 cells by immunofluorescence (Fig. 1B). Treatment with TGFβ and EGF promoted an elongated cellular morphology, the appearance of F-actin fibers, and decreased E-cadherin intensity. U0126 addition prevented E-cadherin loss and promoted E-cadherin localization at cell-cell junctions.

MEK inhibition promotes epithelial phenotypes in NSCLC cells

We next explored the ability of MEK inhibition alone to promote epithelial characteristics in H1666 cells. As seen when combined with TGFβ and EGF, U0126 promoted E-cadherin localization at cell-cell junctions (Fig. 2A). MEK inhibition also antagonized H1666 wound healing in a treatment timedependent manner (Fig. 2B, Supplementary Fig. S3). While U0126 inhibited ERK phosphorylation within 1 hr of addition (Supplementary Fig. S1), U0126 treatment for the duration of the scratch assay (10 hrs) did not significantly affect wound closure rate (“at scratch” condition versus DMSO in Fig. 2B). Wound closure rate decreased significantly with 1 day of U0126 pre-treatment and was nearly zero with four days of pre-treatment. Western blots of lysates created in parallel revealed that E-cadherin expression increased and vimentin expression decreased with increasing U0126 exposure time, consistent with the time-dependent changes in wound closure rate (Fig. 2C, Supplementary Fig. S3). U0126-mediated changes in wound healing migration were further confirmed by assessing migration across Transwell inserts (Fig. 2D).

Chronic MEK inhibition sensitizes NSCLC cells to EGFR inhibition on a time scale consistent with changes in epithelial and mesenchymal markers

Since epithelial characteristics have been connected to EGFR dependence in NSCLC (14, 21), we explored the ability of MEK inhibition to increase sensitivity to gefitinib (Fig. 3). As described in *Materials and Methods*, H1666 cells were maintained in 10 μM U0126 or

DMSO (control) for up to 3 weeks. Throughout the 3-week period, cells were evaluated for death response to gefitinib. Without U0126 pre-treatment, 2 days of EGFR and MEK co-inhibition led to only 7% cell death in H1666, but this more than doubled with 3 days of U0126 pre-treatment (Fig. 3A, Supplementary Fig. S4A). This enhancement further increased with additional U0126 pre-treatment time, reaching a maximum at 11 days. Increased cellular sensitivity to gefitinib was accompanied by increased E-cadherin expression (Fig. 3B, Supplementary Fig. S4B). Beyond 11 days, the synergistic effect began to decrease, which was accompanied by increased fibronectin expression and decreased E-cadherin expression. Similar effects were observed in H1666 cells using CI- 1040 (Supplementary Fig. S4C).

H358 and H322 cells and the breast cancer cell line SKBR3 were also evaluated for response to gefitinib following chronic MEK inhibition (Supplementary Fig. S5). H358 cells harbor a *KRAS* mutation and are ERK-addicted (30). Not surprisingly therefore, H358 response to gefitinib was not augmented by U0126 pre-treatment. However, H322 and SKBR3 cells were sensitized to EGFR inhibition with 5 days of U0126 exposure, suggesting fairly broad applicability of this strategy.

We also probed the reversibility of the effects of chronic MEK inhibition in H1666 cells (Fig. 3C-E, Supplementary Fig. S6). After 7 days, a fraction of cells was split from the U0126 culture and maintained in media containing DMSO (control). This “U0126 removal” culture was subsequently plated in parallel with the cells maintained in U0126. After 7 days of U0126 exposure, removal from U0126 for 4 days completely reversed changes in cellular sensitivity to gefitinib and epithelial and mesenchymal marker expression (Fig. 3C, D, Supplementary Fig. S6A).

Stem cell-like sub-populations with intrinsic therapeutic resistance are found within tumors (20, 31) and are typically identified as $CD44^{high}/CD24^{low}$ (20) or E-$cadherin^{low}$ (32). $CD44^{high}/CD24^{low}$ enrichment from heterogeneous cultures promotes mesenchymal behaviors including resistance to EGFR inhibitors (20). Using flow cytometry, we measured the shift in the $CD44^{high}/CD24^{low}$ sub-population with U0126 addition and subsequent removal (Fig. 3E, Supplementary Fig. S6B). U0126-treated cells had fewer $CD44^{high}/CD24^{low}$ cells and more $CD44^{low}/CD24^{high}$ cells than controls. As with epithelial/mesenchymal marker expression, U0126 removal for four days reversed the effect on the $CD44^{low}/CD24^{high}$ population.

$KRAS^{12V}$-mediated ERK activation promotes EMT

To further probe the connection between ERK activity and EMT, we expressed $KRAS^{12V}$ in H1666 cells. This produced an anticipated increase in ERK phosphorylation and increased vimentin expression (Fig. 4A). Gefitinib and U0126 promoted an epithelial shift in control cells, as determined by western blot and wound closure measurements (Fig. 4A, B). $KRAS^{12V}$ promoted maintenance of ERK phosphorylation in response to gefitinib and largely prevented gefitinib-mediated changes in marker expression and wound closure (Fig. 4A, B). Importantly, the effects of $KRAS^{12V}$ were MEK-dependent, as demonstrated by the effects of U0126 (Fig. 4).

MEK inhibition antagonizes mesenchymal phenotypes and acquired resistance to EGFR inhibition in an EGFR mutant-expressing cell line

We tested the effects of chronic MEK inhibition in a panel of cell lines derived from PC9 cells, which express $EGFR^{delE746\_A750}$ and are gefitinib sensitive. In parental PC9 cells, MEK inhibition prevented TGFβ-mediated EMT and drove changes in epithelial/

mesenchymal marker expression and wound healing consistent with the effects observed in H1666 cells (Fig. 5, Supplementary Fig. S7).

A previous study derived PC9 cells that acquired gefitinib resistance through $EGFR^{T790M}$ mutation (28). Another cell line was then derived from these cells with secondary resistance to the irreversible EGFR inhibitor WZ4002, which potently inhibits $EGFR^{T790M}$ (28, 33). WZ4002 resistance arose through *ERK2* amplification. We used these gefitinib-resistant (GR) and WZ4002-resistant (WZR) clones to examine the effects of ERK2 activity, which has been tied to EMT in non-transformed cells (26). WZR cells displayed a more mesenchymal marker expression pattern than parental or GR cells, with increased fibronectin and vimentin expression and decreased E-cadherin expression (Fig. 6A). WZR cells were also more migratory than GR cells as measured by wound closure and Transwell migration (Fig. 6B, C).

The effects of chronic MEK inhibition were tested in GR and WZR cells, using a higher U0126 concentration for WZR because of the *ERK2* amplification. Death response to cotreatment was enhanced by approximately two-fold with three days of U0126 pre-treatment in both cell lines (Fig. 7A, Supplementary Fig. S8A,B). As in H1666 cells, sufficiently long U0126 exposure resulted in an eventual decrease in augmented response to EGFR inhibition. Increased sensitivity to gefitinib correlated with reduced vimentin expression and slight increases in E-cadherin expression, and the eventual decrease in augmentation was accompanied by increased fibronectin expression in WZR cells (fibronectin was not detectable in GR cells) (Fig. 7B, Supplementary Fig. S8C).

DISCUSSION

We characterized the role of ERK in regulating EMT in NSCLC cells. MEK inhibition prevented TGFβ-induced EMT in NSCLC cell lines expressing wild-type EGFR and KRAS (H1666 and H322), wild-type EGFR and mutant KRAS (H358), or mutant EGFR (PC9). This suggests a general role for ERK in promoting mesenchymal characteristics across typical NSCLC cell types. MEK inhibition also antagonized mesenchymal-associated characteristics including migration, resistance to EGFR inhibition, and $CD44^{high}/CD24^{low}$ expression.

The role of ERK in EMT has been explored in other cell types. ERK is an established determinant of EMT in non-transformed cells (23, 34–36), with ERK2 specifically implicated as an EMT driver (26, 27, 37). This is consistent with findings in breast cancer (38), where MEK inhibition reverses miR-21-mediated EMT, and with studies of phosphatases regulating ERK (i.e., MKP3, PTPN14, and SHP2) (39–41), which also suggest a connection between ERK activity and EMT.

A number of factors regulate ERK activity in NSCLC cells. We previously demonstrated a connection of impaired mutant EGFR endocytosis with a diminished functional role of SHP2 and impaired ERK activity (29, 42). More recently, in collaboration with others, we identified a coupling between *ERK2* amplification and increased EGFR endocytosis in the WZ4002-resistant PC9 cells used here (28). Interestingly, inhibiting EGFR endocytosis in WZ4002-resistant cells reduced ERK phosphorylation and promoted an epithelial marker expression pattern (Supplementary Fig. S9), drawing a potential connection between EGFR endocytosis and EMT. More recently, Sprouty2 has been shown to promote ERK activity in NSCLC cells with or without *EGFR* mutations (43).

Of course, *KRAS* mutations may also promote ERK activity in NSCLC. In H1666 cells, $KRAS^{12V}$-driven ERK activity promoted mesenchymal marker expression and resistance to

gefitinib-mediated MET changes. These findings are generally consistent with studies connecting oncogenic HRAS or KRAS mutants with EMT in mammary epithelia (26), pancreatic cancer (27, 30), and lung cancer (30). The MEK dependence of our observations with $KRAS^{12V}$ may support exploration of MEK and ERK inhibitors in NSCLCs with KRAS mutation.

In addition to promoting epithelial marker expression, MEK inhibition promoted response to EGFR inhibition. Some studies have suggested the efficacy of EGFR and MEK coinhibition in gastric cancer (44) and pancreatic cancer cells (45), and current clinical trials are testing erlotinib combined with MEK inhibitors in NSCLC. In light of this, it is worth noting that the effects we observed with MEK inhibition occurred on a time scale that was much longer than that for ERK inhibition and more consistent with changes in epithelial and mesenchymal marker expression. This may suggest considering a clinical scheduling approach wherein a MEK inhibitor is initially used alone to promote an epithelial phenotype, followed by addition of an EGFR inhibitor. An analogous staggered drug scheduling approach was effective in triple negative breast cancer cells which were sensitized to doxorubicin by erlotinib pre-treatment *in vitro* and in mouse tumor xenografts (9). Applying this basic concept to future clinical trial design may allow for lower MEK inhibitor doses to curb toxicities (46) and promote response to EGFR inhibitors. Given that the time windows for augmented response to gefitinib and the useful concentrations of U0126 were variable among cell lines, it will of course be important first to examine this strategy in pre-clinical animal models to assess general efficacy in an *in vivo* setting and optimize timing and dosing.

We note as well that some recent data suggests that MET is required for efficient colonization of distant metastases (47, 48). Thus, in evaluating different potential strategies for driving MET, the potential to drive proliferation of metastases will have to be weighed against potential ability to kill tumor cells. ERK may be an especially attractive target in this regard. In at least one study, ERK inhibition through microRNA-mediated reduction of SHP2 (a positive regulator of ERK signaling) reduced metastases in an *in vivo* breast cancer model (49), which was due to SHP2's simultaneous regulation of proliferation, invasion, and transcription factor expression. Thus, promoting MET through ERK inhibition, which should additionally inhibit cellular proliferation, may mitigate risks associated with proliferation of micrometastases.

In all three cell lines we tested for effects of chronic MEK inhibition, enhanced gefitinib response eventually decreased. Though initially unresponsive to U0126, U0126-cultured cells displayed noticeable cell death at mid-range time points (partially reflected by cell death measurements for U0126-only samples in Figs. 3 and 7). This could result in selection for U0126-resistant cells over time. Since the fraction of $CD44^{high}/CD24^{low}$ cells in U0126-treated cultures remained low at time points when resistance was observed (Fig. 3C,E), the potentially inherently resistant population was apparently not $CD44^{high}/CD24^{low}$. Alternatively, resistance could arise from adaptation of the entire cell population, for example through increased fibronectin-mediated signaling, which has been linked to AKT activation and docetaxel resistance in ovarian and breast cancer cells (50). Indeed, in all cases, the eventual drop in augmented response to gefitinib was accompanied by increased fibronectin expression. Future work should consider effectors of fibronectin-mediated signaling as signaling nodes whose inhibition may augment EGFR inhibitor response.

While our data suggest potential relevance of our findings to *de novo* and acquired EGFR inhibitor resistance, responsiveness to chronic MEK inhibition was not uniform among cell lines, which could result from any of the numerous differences in initial conditions among NSCLC cell lines. For example, while H1666 cells express wild-type EGFR and KRAS,

they also express the low-activity G446V BRAF mutant (51), which could influence their death response to MEK inhibition. In the future, therefore, investigating the cellular initial conditions that may determine responsiveness to this approach and identifying alternative signaling nodes whose inhibition may result in more stable maintenance of an epithelial cell type will also be important.

Supplementary Material

Refer to Web version on PubMed Central for supplementary material.

Acknowledgments

The authors thank Drs. Pasi Jänne, Douglas Lauffenburger, Deepak Nihalani, and Russ Carstens for generously providing reagents. The authors also thank Calixte Monast, Chris Furcht, and Alice Walsh for technical assistance and guidance.

Financial Support

This work was supported in part by the National Institutes of Health under Ruth L. Kirschstein National Research Service Award 2T32HL007954 from the NIH-NHLBI. This material is also based upon work supported by the National Science Foundation Graduate Research Fellowship under Grant No. DGE-0822.

References

1. Lynch TJ, Bell DW, Sordella R, Gurubhagavatula S, Okimoto RA, Brannigan BW, et al. Activating mutations in the epidermal growth factor receptor underlying responsiveness of non-small-cell lung cancer to gefitinib. N Engl J Med. 2004; 350:2129–2139. [PubMed: 15118073]
2. Sordella R, Bell DW, Haber DA, Settleman J. Gefitinib-sensitizing EGFR mutations in lung cancer activate anti-apoptotic pathways. Science. 2004; 305:1163–1167. [PubMed: 15284455]
3. Kobayashi S, Boggon TJ, Dayaram T, Janne PA, Kocher O, Meyerson M, et al. EGFR mutation and resistance of non-small-cell lung cancer to gefitinib. N Engl J Med. 2005; 352:786–792. [PubMed: 15728811]
4. Pao W, Miller VA, Politi KA, Riely GJ, Somwar R, Zakowski MF, et al. Acquired resistance of lung adenocarcinomas to gefitinib or erlotinib is associated with a second mutation in the EGFR kinase domain. PLoS Med. 2005; 2:e73. [PubMed: 15737014]
5. Engelman JA, Zejnullahu K, Mitsudomi T, Song Y, Hyland C, Park JO, et al. MET amplification leads to gefitinib resistance in lung cancer by activating ERBB3 signaling. Science. 2007; 316:1039–1043. [PubMed: 17463250]
6. Blumenschein GR Jr, Paulus R, Curran WJ, Robert F, Fossella F, Werner-Wasik M, et al. Phase II study of cetuximab in combination with chemoradiation in patients with stage IIIA/B non-small-cell lung cancer: RTOG 0324. J Clin Oncol. 2011; 29:2312–2318. [PubMed: 21555682]
7. Spigel DR, Burris HA 3rd, Greco FA, Shipley DL, Friedman EK, Waterhouse DM, et al. Randomized, double-blind, placebo-controlled, phase II trial of sorafenib and erlotinib or erlotinib alone in previously treated advanced non-small-cell lung cancer. J Clin Oncol. 2011; 29:2582–2589. [PubMed: 21576636]
8. Xu L, Kikuchi E, Xu C, Ebi H, Ercan D, Cheng KA, et al. Combined EGFR/MET or EGFR/HSP90 Inhibition Is Effective in the Treatment of Lung Cancers Codriven by Mutant EGFR Containing T790M and MET. Cancer Res. 2012; 72:3302–3311. [PubMed: 22552292]
9. Lee MJ, Ye AS, Gardino AK, Heijink AM, Sorger PK, MacBeath G, et al. Sequential application of anticancer drugs enhances cell death by rewiring apoptotic signaling networks. Cell. 2012; 149:780–794. [PubMed: 22579283]
10. Kalluri R, Weinberg RA. The basics of epithelial-mesenchymal transition. J Clin Invest. 2009; 119:1420–1428. [PubMed: 19487818]
11. Zavadil J, Bottinger EP. TGF-beta and epithelial-to-mesenchymal transitions. Oncogene. 2005; 24:5764–5774. [PubMed: 16123809]

12. Garofalo M, Romano G, Di Leva G, Nuovo G, Jeon YJ, Ngankeu A, et al. EGFR and MET receptor tyrosine kinase-altered microRNA expression induces tumorigenesis and gefitinib resistance in lung cancers. Nat Med. 2011; 18:74–82. [PubMed: 22157681]

13. Thomson S, Petti F, Sujka-Kwok I, Epstein D, Haley JD. Kinase switching in mesenchymal-like non-small cell lung cancer lines contributes to EGFR inhibitor resistance through pathway redundancy. Clin Exp Metastasis. 2008; 25:843–854. [PubMed: 18696232]

14. Yauch RL, Januario T, Eberhard DA, Cavet G, Zhu W, Fu L, et al. Epithelial versus mesenchymal phenotype determines in vitro sensitivity and predicts clinical activity of erlotinib in lung cancer patients. Clin Cancer Res. 2005; 11:8686–8698. [PubMed: 16361555]

15. Shrader M, Pino MS, Brown G, Black P, Adam L, Bar-Eli M, et al. Molecular correlates of gefitinib responsiveness in human bladder cancer cells. Mol Cancer Ther. 2007; 6:277–285. [PubMed: 17237287]

16. Frederick BA, Helfrich BA, Coldren CD, Zheng D, Chan D, Bunn PA Jr, et al. Epithelial to mesenchymal transition predicts gefitinib resistance in cell lines of head and neck 19 squamous cell carcinoma and non-small cell lung carcinoma. Mol Cancer Ther. 2007; 6:1683–1691. [PubMed: 17541031]

17. Maseki S, Ijichi K, Tanaka H, Fujii M, Hasegawa Y, Ogawa T, et al. Acquisition of EMT phenotype in the gefitinib-resistant cells of a head and neck squamous cell carcinoma cell line through Akt/GSK-3beta/snail signalling pathway. Br J Cancer. 2012; 106:1196–1204. [PubMed: 22315058]

18. Yin T, Wang C, Liu T, Zhao G, Zha Y, Yang M. Expression of snail in pancreatic cancer promotes metastasis and chemoresistance. J Surg Res. 2007; 141:196–203. [PubMed: 17583745]

19. Li X, Lewis MT, Huang J, Gutierrez C, Osborne CK, Wu MF, et al. Intrinsic resistance of tumorigenic breast cancer cells to chemotherapy. J Natl Cancer Inst. 2008; 100:672–679. [PubMed: 18445819]

20. Yao Z, Fenoglio S, Gao DC, Camiolo M, Stiles B, Lindsted T, et al. TGF-beta IL-6 axis mediates selective and adaptive mechanisms of resistance to molecular targeted therapy in lung cancer. Proc Natl Acad Sci U S A. 2010; 107:15535–15540. [PubMed: 20713723]

21. Witta SE, Gemmill RM, Hirsch FR, Coldren CD, Hedman K, Ravdel L, et al. Restoring Ecadherin expression increases sensitivity to epidermal growth factor receptor inhibitors in lung cancer cell lines. Cancer Res. 2006; 66:944–950. [PubMed: 16424029]

22. Zhang Z, Lee JC, Lin L, Olivas V, Au V, LaFramboise T, et al. Activation of the AXL kinase causes resistance to EGFR-targeted therapy in lung cancer. Nat Genet. 2012; 44:852–860. [PubMed: 22751098]

23. Grande M, Franzen A, Karlsson JO, Ericson LE, Heldin NE, Nilsson M. Transforming growth factor-beta and epidermal growth factor synergistically stimulate epithelial to mesenchymal transition (EMT) through a MEK-dependent mechanism in primary cultured pig thyrocytes. J Cell Sci. 2002; 115:4227–4236. [PubMed: 12376555]

24. Xie L, Law BK, Chytil AM, Brown KA, Aakre ME, Moses HL. Activation of the Erk pathway is required for TGF-beta1-induced EMT in vitro. Neoplasia. 2004; 6:603–610. [PubMed: 15548370]

25. Zavadil J, Bitzer M, Liang D, Yang YC, Massimi A, Kneitz S, et al. Genetic programs of epithelial cell plasticity directed by transforming growth factor-beta. Proc Natl Acad Sci U S A. 2001; 98:6686–6691. [PubMed: 11390996]

26. Shin S, Dimitri CA, Yoon SO, Dowdle W, Blenis J. ERK2 but not ERK1 induces epithelial-to-mesenchymal transformation via DEF motif-dependent signaling events. Mol Cell. 2010; 38:114–127. [PubMed: 20385094]

27. Botta GP, Reginato MJ, Reichert M, Rustgi AK, Lelkes PI. Constitutive K-RasG12D activation of ERK2 specifically regulates 3D invasion of human pancreatic cancer cells via MMP-1. Mol Cancer Res. 2011; 10:183–196. [PubMed: 22160930]

28. Ercan D, Xu C, Yanagita M, Monast CS, Pratilas CA, Montero J, et al. Reactivation of ERK Signaling Causes Resistance to EGFR Kinase Inhibitors. Cancer Discov. 2012; 2:934–947. [PubMed: 22961667]

29. Lazzara MJ, Lane K, Chan R, Jasper PJ, Yaffe MB, Sorger PK, et al. Impaired SHP2-mediated extracellular signal-regulated kinase activation contributes to gefitinib sensitivity of lung cancer

cells with epidermal growth factor receptor-activating mutations. Cancer Res. 2010; 70:3843–3850. [PubMed: 20406974]

30. Singh A, Greninger P, Rhodes D, Koopman L, Violette S, Bardeesy N, et al. A gene expression signature associated with "K-Ras addiction" reveals regulators of EMT and tumor cell survival. Cancer Cell. 2009; 15:489–500. [PubMed: 19477428]
31. Basu D, Nguyen TT, Montone KT, Zhang G, Wang LP, Diehl JA, et al. Evidence for mesenchymal-like sub-populations within squamous cell carcinomas possessing chemoresistance and phenotypic plasticity. Oncogene. 2010; 29:4170–4182. [PubMed: 20498638]
32. Basu D, Montone KT, Wang LP, Gimotty PA, Hammond R, Diehl JA, et al. Detecting and targeting mesenchymal-like subpopulations within squamous cell carcinomas. Cell Cycle. 2011; 10:2008–2016. [PubMed: 21558812]
33. Zhou W, Ercan D, Chen L, Yun CH, Li D, Capelletti M, et al. Novel mutant-selective EGFR kinase inhibitors against EGFR T790M. Nature. 2009; 462:1070–1074. [PubMed: 20033049]
34. Janda E, Lehmann K, Killisch I, Jechlinger M, Herzig M, Downward J, et al. Ras and TGF[beta] cooperatively regulate epithelial cell plasticity and metastasis: dissection of Ras signaling pathways. J Cell Biol. 2002; 156:299–313. [PubMed: 11790801]
35. Lehmann K, Janda E, Pierreux CE, Rytomaa M, Schulze A, McMahon M, et al. Raf induces TGFbeta production while blocking its apoptotic but not invasive responses: a mechanism leading to increased malignancy in epithelial cells. Genes Dev. 2000; 14:2610–2622. [PubMed: 11040215]
36. Peinado H, Quintanilla M, Cano A. Transforming growth factor beta-1 induces snail transcription factor in epithelial cell lines: mechanisms for epithelial mesenchymal transitions. J Biol Chem. 2003; 278:21113–21123. [PubMed: 12665527]
37. von Thun A, Birtwistle M, Kalna G, Grindlay J, Strachan D, Kolch W, et al. ERK2 drives tumour cell migration in three-dimensional microenvironments by suppressing expression of Rab17 and liprin-beta2. J Cell Sci. 2012; 125:1465–1477. [PubMed: 22328529]
38. Han M, Liu M, Wang Y, Chen X, Xu J, Sun Y, et al. Antagonism of miR-21 Reverses Epithelial-Mesenchymal Transition and Cancer Stem Cell Phenotype through AKT/ERK1/2 Inactivation by Targeting PTEN. PLoS One. 2012; 7:e39520. [PubMed: 22761812]
39. Liu X, Yang N, Figel SA, Wilson KE, Morrison CD, Gelman IH, et al. PTPN14 interacts with and negatively regulates the oncogenic function of YAP. Oncogene. 2012
40. Wong VC, Chen H, Ko JM, Chan KW, Chan YP, Law S, et al. Tumor suppressor dualspecificity phosphatase 6 (DUSP6) impairs cell invasion and epithelial-mesenchymal transition (EMT)-associated phenotype. Int J Cancer. 2011; 130:83–95. [PubMed: 21387288]
41. Zhou XD, Agazie YM. Inhibition of SHP2 leads to mesenchymal to epithelial transition in breast cancer cells. Cell Death Differ. 2008; 15:988–996. [PubMed: 18421299]
42. Furcht CM, Munoz Rojas AR, Nihalani D, Lazzara MJ. Diminished functional role and altered localization of SHP2 in non-small cell lung cancer cells with EGFR-activating mutations. Oncogene. 2013; 32:2346–2355. 55 e1–55 e10. [PubMed: 22777356]
43. Walsh AM, Lazzara MJ. Regulation of EGFR trafficking and cell signaling by Sprouty2 and MIG6 in lung cancer cells. J Cell Sci. 2013
44. Yoon YK, Kim HP, Han SW, Hur HS, Oh do Y, Im SA, et al. Combination of EGFR and MEK1/2 inhibitor shows synergistic effects by suppressing EGFR/HER3-dependent AKT activation in human gastric cancer cells. Mol Cancer Ther. 2009; 8:2526–2536. [PubMed: 19755509]
45. Diep CH, Munoz RM, Choudhary A, Von Hoff DD, Han H. Synergistic effect between erlotinib and MEK inhibitors in KRAS wild-type human pancreatic cancer cells. Clin Cancer Res. 2011; 17:2744–2756. [PubMed: 21385921]
46. Wang D, Boerner SA, Winkler JD, LoRusso PM. Clinical experience of MEK inhibitors in cancer therapy. Biochim Biophys Acta. 2007; 1773:1248–1255. [PubMed: 17194493]
47. Celia-Terrassa T, Meca-Cortes O, Mateo F, de Paz AM, Rubio N, Arnal-Estape A, et al. Epithelial-mesenchymal transition can suppress major attributes of human epithelial tumorinitiating cells. J Clin Invest. 2012; 122:1849–1868. [PubMed: 22505459]
48. Tsai JH, Donaher JL, Murphy DA, Chau S, Yang J. Spatiotemporal regulation of epithelialmesenchymal transition is essential for squamous cell carcinoma metastasis. Cancer Cell. 2012; 22:725–736. [PubMed: 23201165]

49. Aceto N, Sausgruber N, Brinkhaus H, Gaidatzis D, Martiny-Baron G, Mazzarol G, et al. Tyrosine phosphatase SHP2 promotes breast cancer progression and maintains tumorinitiating cells via activation of key transcription factors and a positive feedback signaling loop. Nat Med. 2012; 18:529–537. [PubMed: 22388088]

50. Xing H, Weng D, Chen G, Tao W, Zhu T, Yang X, et al. Activation of fibronectin/PI- 3K/Akt2 leads to chemoresistance to docetaxel by regulating survivin protein expression in ovarian and breast cancer cells. Cancer Lett. 2008; 261:108–119. [PubMed: 18171600]

51. Pratilas CA, Hanrahan AJ, Halilovic E, Persaud Y, Soh J, Chitale D, et al. Genetic predictors of MEK dependence in non-small cell lung cancer. Cancer Res. 2008; 68:9375–9383. [PubMed: 19010912]

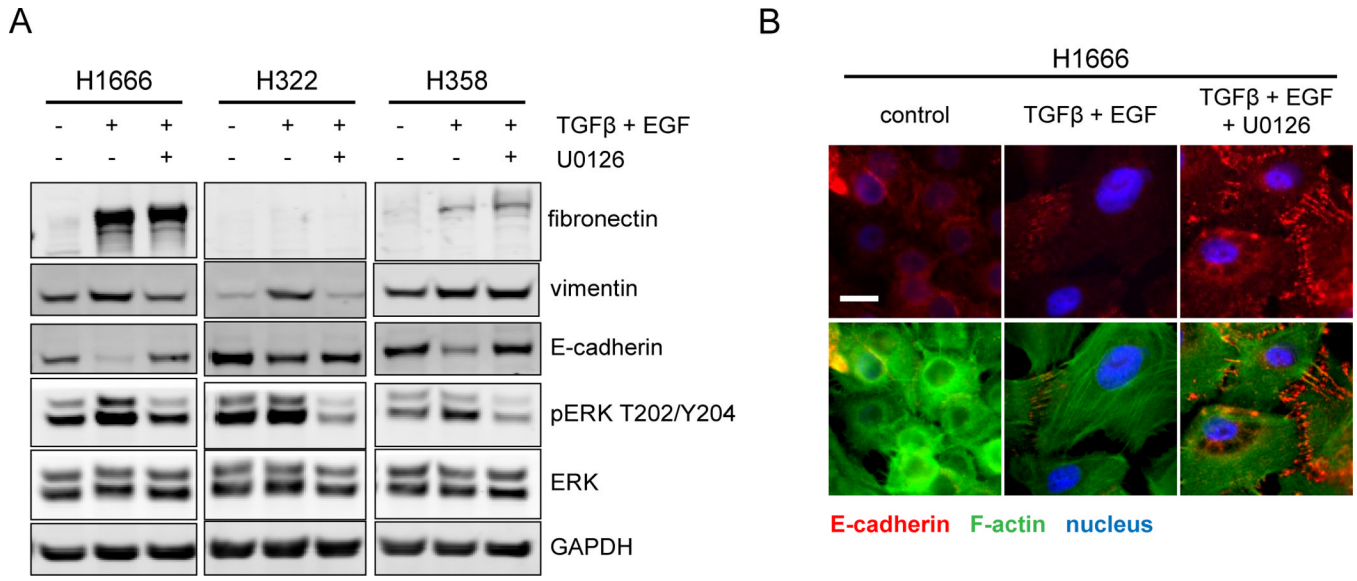

Figure 1. MEK inhibition prevents TGFβ-induced EMT in NSCLC cell lines

(*A*) H1666, H322, and H358 cells were treated for four days with 10 ng/mL TGFβ + 50 ng/mL EGF, TGFβ + EGF and 20 μM U0126, or DMSO (control). Whole cell lysates were analyzed by western blot with antibodies against indicated proteins. Images are representative of at least three independent experiments. (*B*) H1666 cells on glass coverslips were treated as in (*A*), fixed, and stained for E-cadherin, F-actin, and DNA. Images are representative of three replicates from each of two independent experiments. Scale bar = 20 μm.

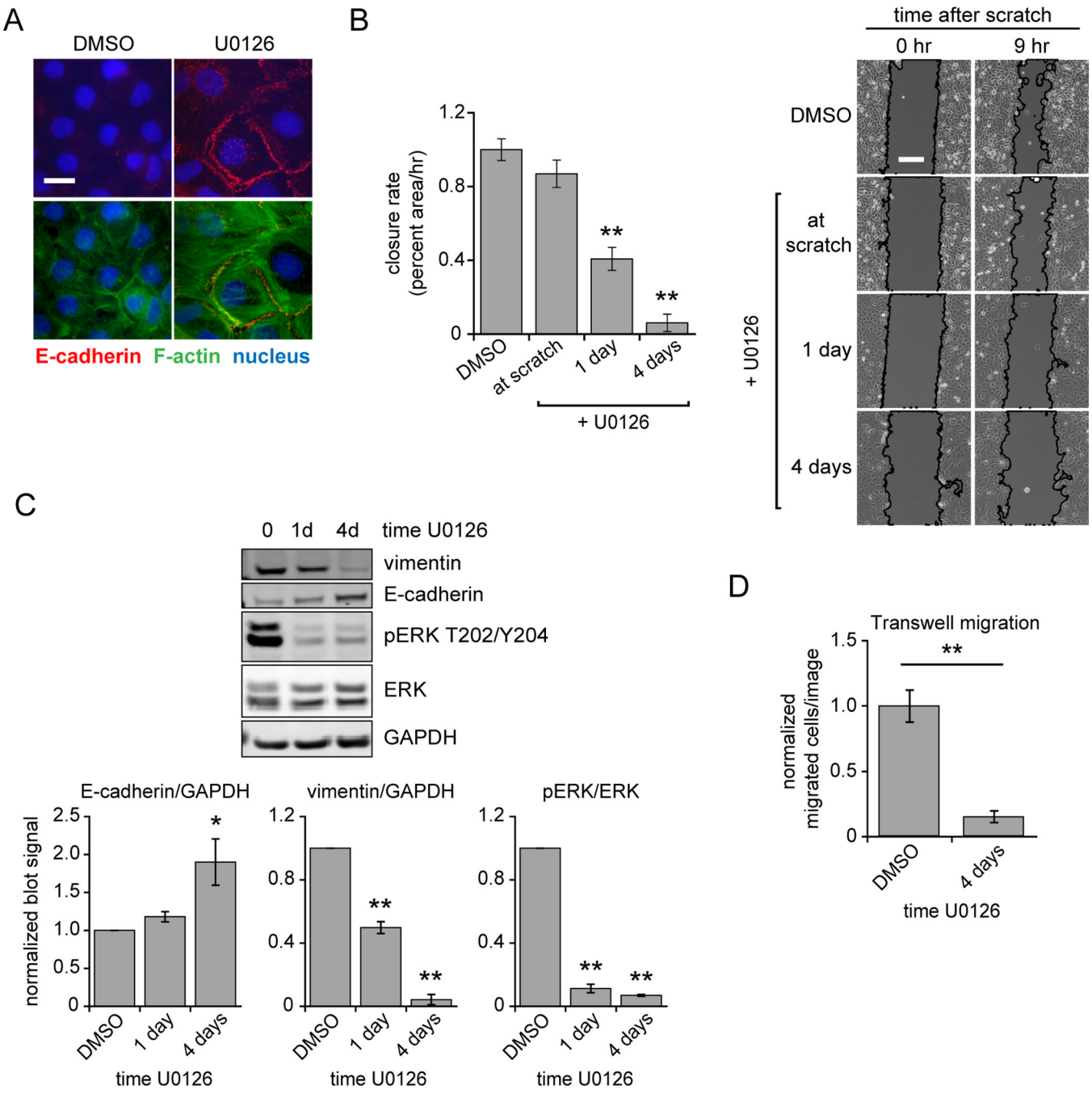

Figure 2. MEK inhibition promotes epithelial characteristics in H1666 cells

(*A*) H1666 cells plated on glass coverslips were treated with 20 μM U0126 for 4 days, fixed, and stained for E-cadherin, F-actin, and DNA. Images are representative of three replicates from each of two independent experiments. Scale bar = 20 μm. (*B*) Wound closure rates were measured for H1666 cells treated with DMSO (control) or 20 μM U0126 at the time of scratch or for 1 or 4 days prior to scratch. Rates normalized to the control condition for triplicate wells from two different platings ($n = 6$) are reported as averages ± s.e.m. Representative phase contrast images are shown, with tracings added to identify open scratch areas. Scale bar = 200 μm. (*C*) Lysates prepared in parallel to (*B*) were analyzed by western blot using antibodies against indicated proteins. Signals normalized to respective

DMSO controls are reported as averages ± s.e.m. (n = 3). (*D*) Transwell migration experiments were performed for H1666 cells pre-treated with DMSO or 20 μM U0126 for 4 days. Counts normalized to DMSO control for duplicate wells from three separate experiments (n = 6) are reported as averages ± s.e.m. * and ** indicate $p < 0.05$ and 0.005, respectively.

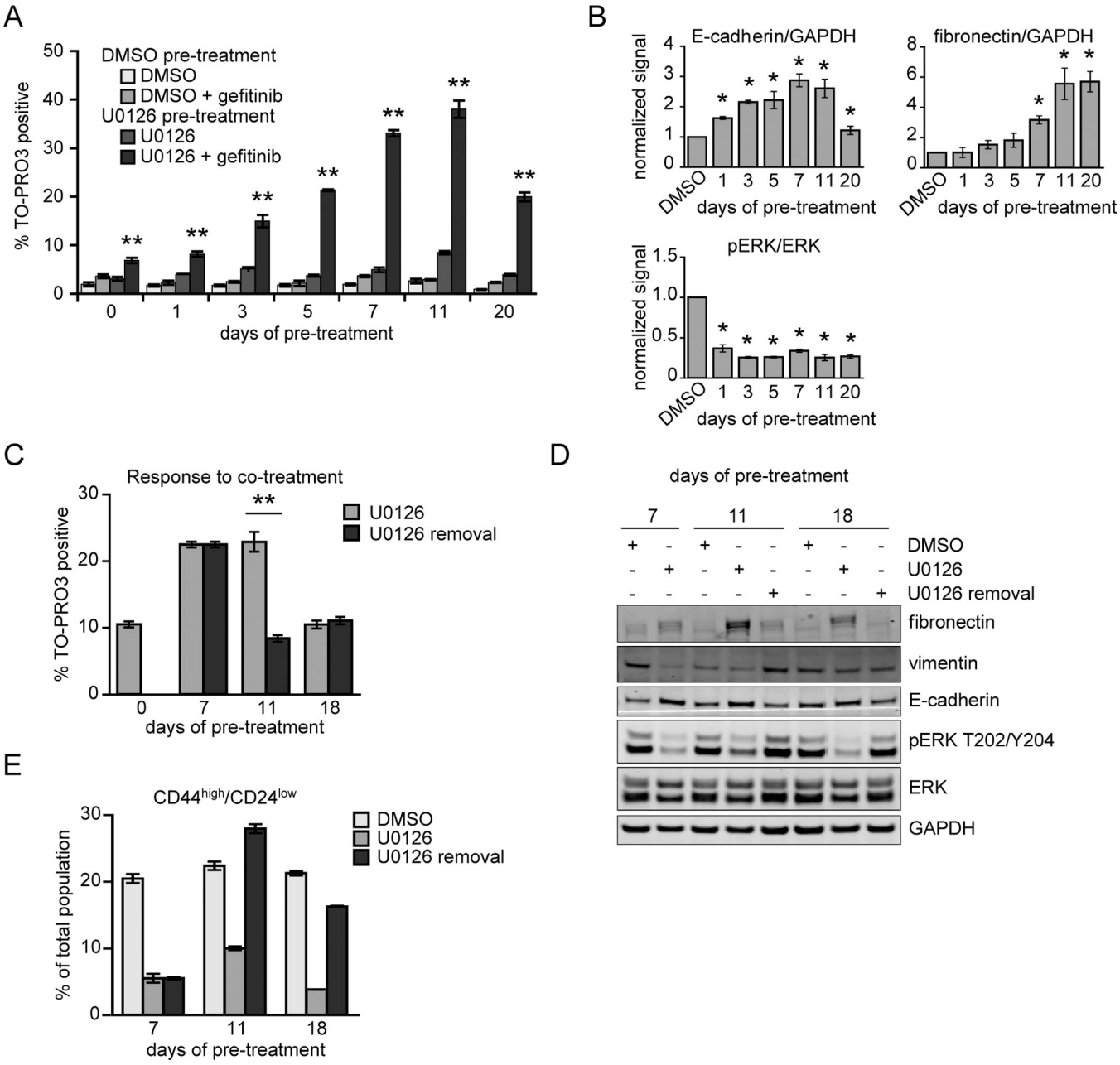

Figure 3. Chronic MEK inhibition sensitizes NSCLC cells to EGFR inhibition

(*A*) H1666 cells were cultured in 10 μM U0126 or DMSO (control) for up to 3 weeks and were evaluated for cell death response to 10 μM gefitinib for various U0126 exposure times. Cell death was measured by flow cytometry for TO-PRO3 permeability 48 hrs after gefitinib addition. Averaged data are shown ± s.e.m. (*n* = 3); significance is relative to any other condition from the same day. (*B*) Lysates prepared in parallel to (*A*), before gefitinib addition, were analyzed by western blot with antibodies against the indicated proteins. Signals normalized to respective DMSO controls are reported as averages ± s.e.m. (*n* = 3). (*C*) Experiments probing the reversibility of U0126-mediated effects were performed as described in *Materials and Methods*. For cells removed from (U0126 removal) or maintained in U0126, response to the same drug co-treatment was assessed by TO-PRO3 permeability at the indicated times. Data are represented as averages ± s.e.m (*n* = 3). (*D* and

E) Reversibility of U0126 effects was assessed by western blot (*D*), using antibodies against indicated proteins, and by flow cytometry for CD44 and CD24 staining (*E*). Blot images are representative of three replicates. Flow cytometry data are represented as averages ± s.e.m. ($n = 3$). In all panels, times indicated reflect the total time of U0126 exposure prior to lysis, gefitinib addition, or staining; * and ** indicate $p < 0.05$ and 0.005, respectively.

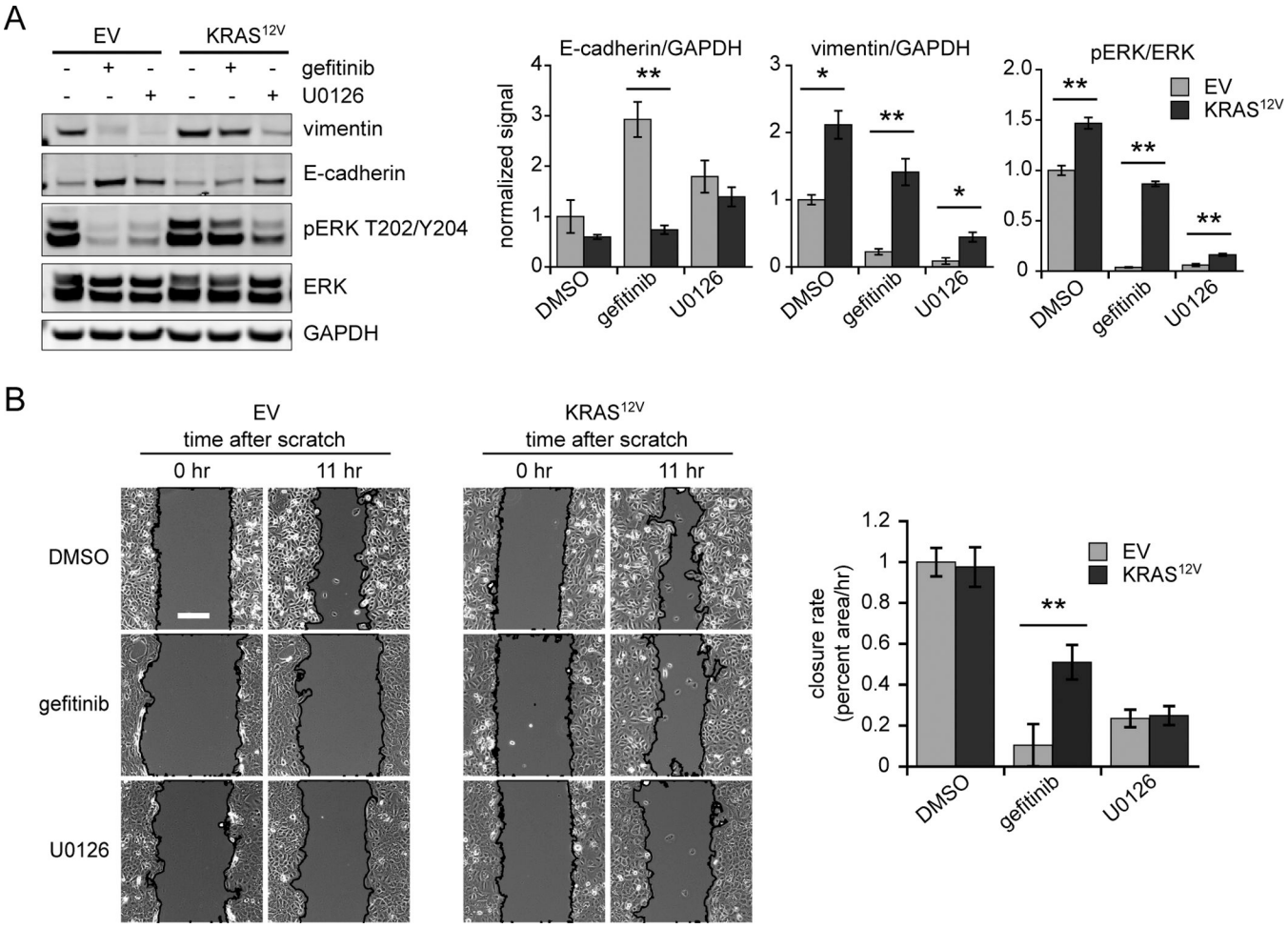

Figure 4. KRAS^{12V} expression promotes mesenchymal characteristics in H1666 cells

(*A*) H1666 cells transduced with KRAS^{12V} or an empty vector control (EV) treated for three days with DMSO, 2 μM gefitinib, or 20 μM U0126 were lysed and analyzed by western blot with antibodies against indicated proteins. Signals normalized to DMSO-treated EV lysates are reported as averages ± s.e.m. (n = 3). (*B*) Wound closure rates were measured for EV- and KRAS^{12V}-transduced cells treated as in panel (*A*). Rates normalized to the EV DMSO control condition are reported as averages ± s.e.m. for triplicate wells from two different platings (n = 6). Representative phase contrast images are shown, with tracings added to identify open scratch areas. Scale bar = 200 μm. * and ** indicate $p < 0.05$ and 0.005, respectively

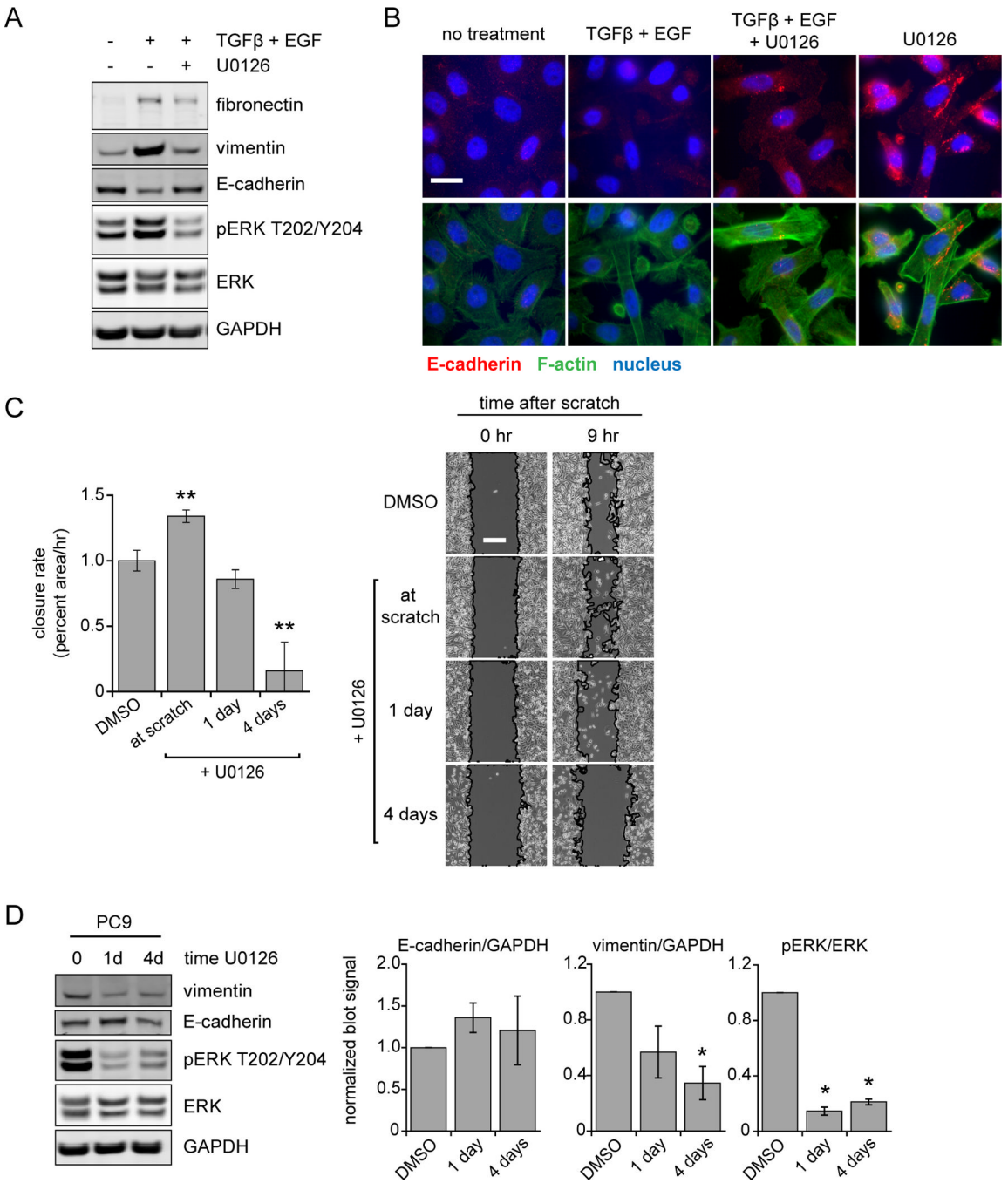

Figure 5. ERK activity determines epithelial/mesenchymal characteristics in an NSCLC cell line with an EGFR-activating mutation

(*A*) Lysates of parental PC9 cells treated for four days with 10 ng/mL TGFβ + 50 ng/mL EGF, TGFβ + EGF and 20 μM U0126, or DMSO (control) were analyzed by western blot with antibodies against indicated proteins. Images are representative of three independent experiments. Scale bar = 20 μm. (*B*) PC9 cells on glass coverslips were treated as in (*A*), fixed, and stained for E-cadherin, F-actin, and DNA. Images are representative of three replicates for each of two independent experiments. (*C*) Wound closure rates were measured for PC9 cells treated with DMSO (control) or 20 μM U0126 at the time of scratch or for 1 or 4 days prior to scratch. Rates normalized to the control condition for triplicate wells from

two different platings ($n = 6$) are reported as averages ± s.e.m. Representative phase contrast images are shown, with tracings added to identify open scratch areas. Scale bar = 200 μm. (*D*) Lysates prepared in parallel to (*C*) were analyzed by western blot using antibodies against indicated proteins. Images are representative of three independent experiments. Signals normalized to respective DMSO controls are reported as averages ± s.e.m. ($n = 3$); * and ** indicate $p < 0.05$ and 0.005, respectively, compared to control.

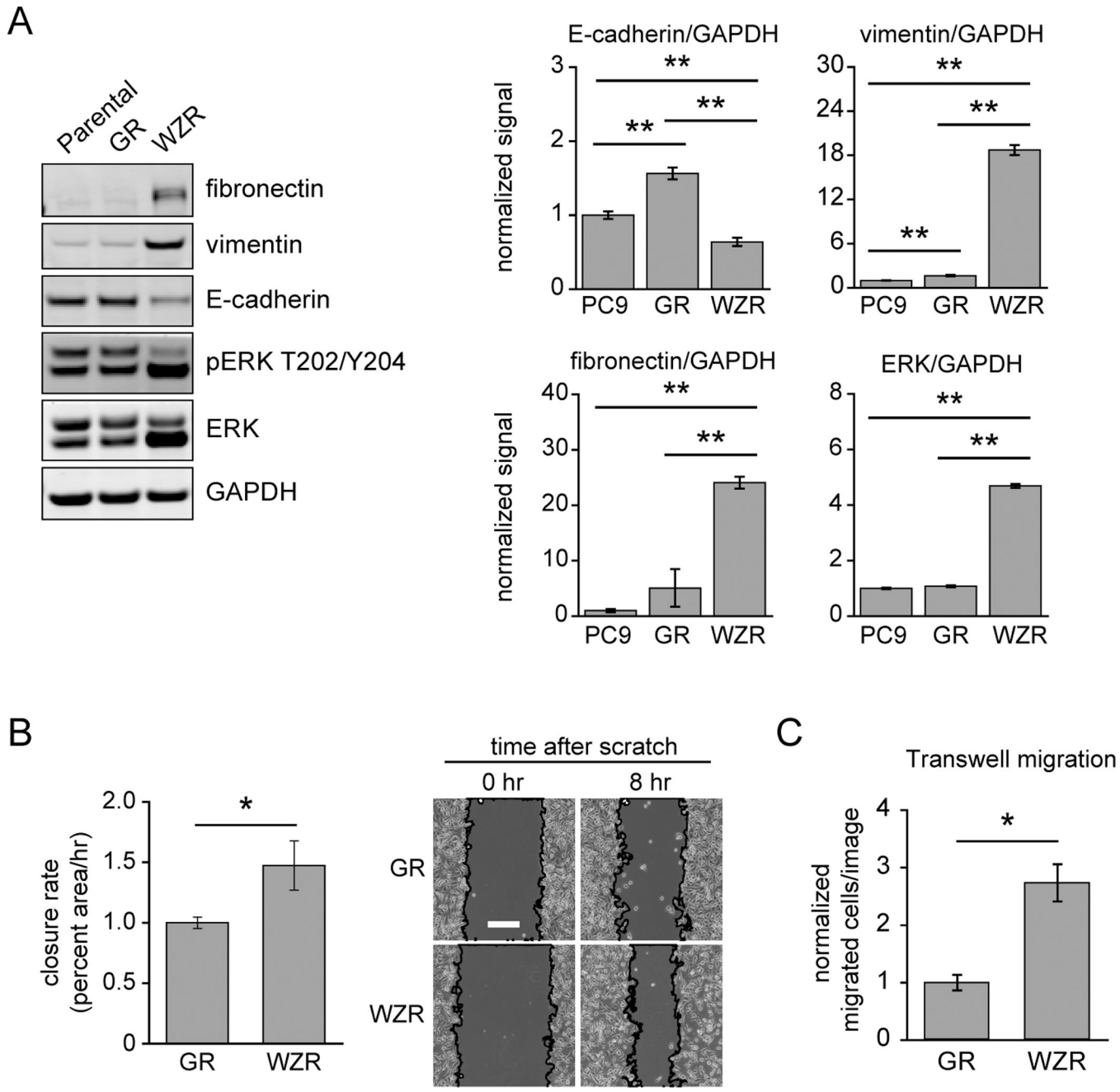

Figure 6. ERK2 amplification promotes mesenchymal characteristics in PC9 cells with acquired resistance to an irreversible EGFR inhibitor

(*A*) Lysates prepared from parental, gefitinib-resistant (GR), and WZ4002-resistant (WZR) PC9 cells grown in complete media were analyzed by western blot using antibodies against indicated proteins. Images are representative of three independent experiments. Densitometry data are shown normalized to PC9 parental signals and are reported as averages ± s.e.m. ($n = 3$); ** indicates $p < 0.01$. (*B*) Wound closure rates were measured for GR and WZR cells. Rates normalized to GR closure rate are reported as averages ± s.e.m. for triplicate wells from each of two different platings ($n = 6$); * indicates $p < 0.05$. Representative phase contrast images are shown, with tracings added to identify open scratch areas. Scale bar = 200 μm. (*C*) Transwell migration measurements were made for

GR and WZR cells. Bars represent averages ± s.e.m. for duplicate wells from three separate experiments ($n = 6$) normalized to GR cells.

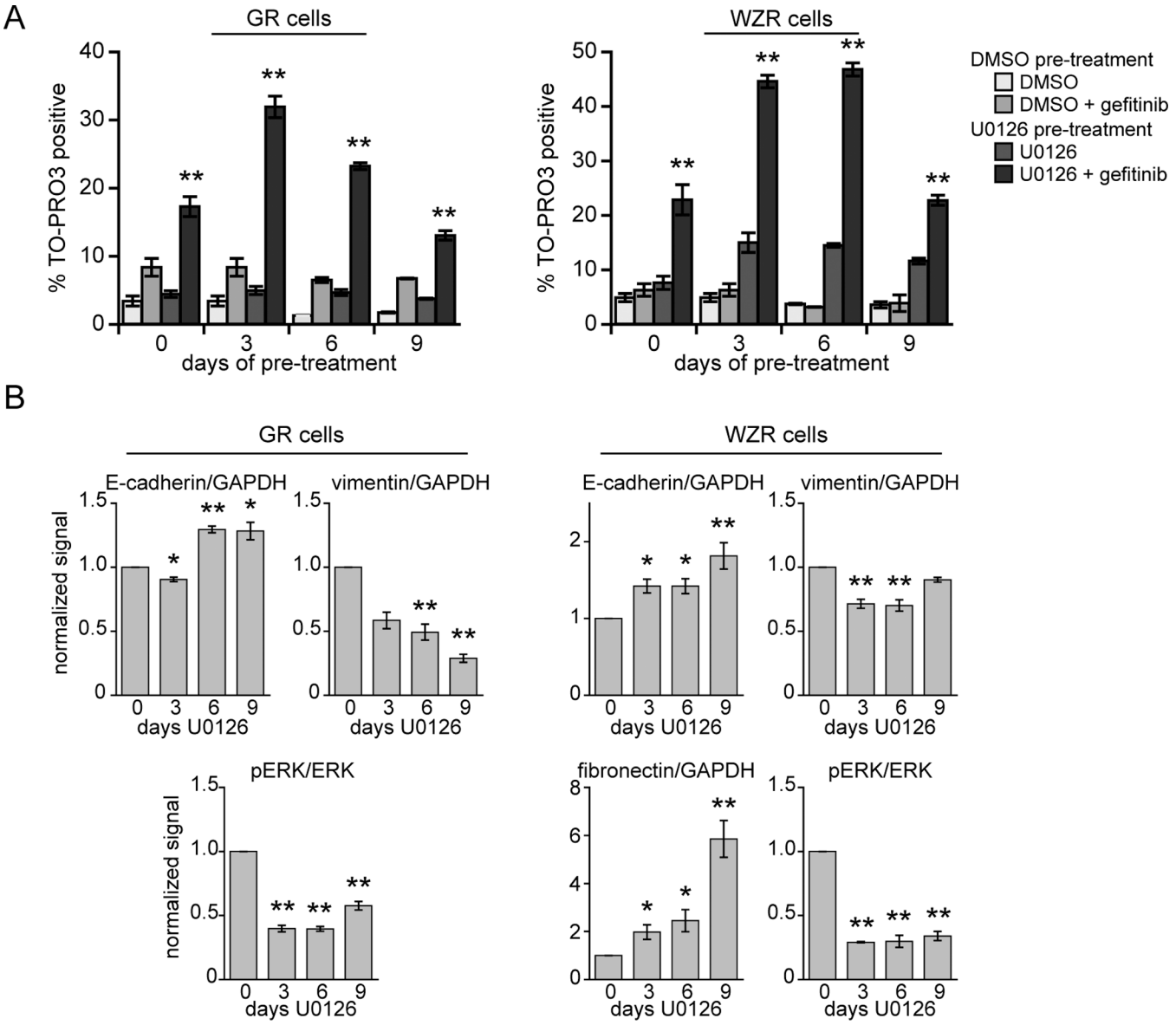

Figure 7. MEK inhibition sensitizes cells with acquired resistance to EGFR inhibitors

(*A*) Gefitinib-resistant (GR) and WZ4002-resistant (WZR) PC9 cells were cultured in 5 μM and 20 μM U0126, respectively, or DMSO (control) for up to 9 days, as described in *Materials and Methods,* and were evaluated for cell death response to 5 μM gefitinib for various U0126 exposure times. Cell death was measured by flow cytometry for TO-PRO3 permeability 48 hrs after gefitinib addition. Time points represent total time exposed to U0126 prior to gefitinib addition or lysis. Data are represented as averages ± s.e.m. ($n = 3$); significance is shown relative to any other condition from the same day. (*B*) GR and WZR cell lysates prepared in parallel to (*A*) were analyzed by western blot using antibodies against indicated proteins. Average signals normalized to respective DMSO controls are reported ± s.e.m ($n = 3$). * and ** indicate $p < 0.05$ and 0.005, respectively.